



STRUCTURAL SCIENCE
CRYSTAL ENGINEERING
MATERIALS

Volume 77 (2021)

Supporting information for article:

Investigation of polar crystalline materials containing hydrochlorothiazide: electron density distribution and optical properties

Joanna Wojnarska, Marlena Gryl, Tomasz Seidler and Katarzyna Marta Stadnicka

S1. Experimental section - Single-crystal X-ray diffraction**Table S1** Crystal data, measurement conditions and structure refinement details. CCDC references: 2091059, 2091060.

	(I)	(II)
Crystal data		
Chemical formula	C ₇ H ₈ N ₃ O ₄ S ₂ Cl	C ₇ H ₈ ClN ₃ O ₄ S ₂ ·C ₅ H ₆ N ₂ ·H ₂ O
Mr	297.73	409.87
Crystal system, space group	Monoclinic, <i>P</i> 2 ₁	Orthorhombic, <i>Pna</i> 2 ₁
Temperature (K)	100	100
<i>a</i> , <i>b</i> , <i>c</i> (Å)	7.3288(1), 8.5032(1), 9.9467(1)	31.6312(6), 7.3092(1), 7.2332(1)
β (°)	111.290(1)	-
<i>V</i> (Å ³)	577.56(1)	1672.31(5)
<i>Z</i>	2	4
Radiation type	Mo <i>K</i> α	Mo <i>K</i> α
μ (mm ⁻¹)	0.70	0.51
Crystal size (mm)	0.30 x 0.27 x 0.08	0.20 x 0.18 x 0.06
Data collection		
Diffractometer	XtaLAB Synergy, Dualflex, HyPix	XtaLAB Synergy, Dualflex, HyPix
Absorption correction	Multi-scan <i>CrysAlis PRO</i> 1.171.40.14e (Rigaku Oxford Diffraction, 2018) Empirical absorption correction using spherical harmonics, implemented in SCALE3 ABSPACK scaling algorithm	Multi-scan <i>CrysAlis PRO</i> 1.171.40.84a (Rigaku Oxford Diffraction, 2020) Empirical absorption correction using spherical harmonics, implemented in SCALE3 ABSPACK scaling algorithm.
<i>T</i> _{min} , <i>T</i> _{max}	0.537, 1.000	0.644, 1.000
No. of measured, independent and	86128, 10895, 9760	78875, 15872, 12319

observed [$I > 2\sigma(I)$] reflections		
R_{int}	0.061	0.045
$(\sin \theta / \lambda)_{\text{max}} (\text{\AA}^{-1})$	1.042	1.055
Refinement		
$R[F^2 > 2\sigma(F^2)]$, $wR(F^2)$, S	0.032, 0.074, 1.04	0.039, 0.083, 1.00
No. of reflections	10895	15872
No. of parameters	166	308
No. of restraints	5	247
H-atom treatment	H atoms treated by a mixture of independent and constrained refinement	H atoms treated by a mixture of independent and constrained refinement
$\Delta\rho_{\text{max}}, \Delta\rho_{\text{min}} (\text{e} \text{\AA}^{-3})$	0.55, -0.55	0.64, -0.29
Absolute structure	Flack x determined using 4113 quotients $[(I+)-(I-)]/[(I+)+(I-)]$ (Parsons, Flack and Wagner, Acta Cryst. B69 (2013) 249-259).	Flack x determined using 4462 quotients $[(I+)-(I-)]/[(I+)+(I-)]$ (Parsons, Flack and Wagner, Acta Cryst. B69 (2013) 249-259).
Absolute structure parameter	-0.019 (18)	-0.006 (14)

Computer programs: *CrysAlis PRO* 1.171.40.14e (Rigaku Oxford Diffraction, 2018), *SHELXT* 2014/5 (Sheldrick, 2014), *SHELXL2018/3* (Sheldrick, 2018), *Mercury* (Macrae, 2008).

S2. Experimental electron density of (I)

S2.1. Details on multipolar refinement

Multipole refinement was carried out using the Hansen–Coppens formalism (Hansen & Coppens, 1978) as implemented in the XD2016 software. (Volkov *et al.*, 2016) The model derived from spherical refinement were used as a starting point. The reflections were merged using Sortav (Blessing, 1997), and only reflections that fulfil criterion $I > 2\sigma(I)$ were included in the refinement process. The positional coordinates of hydrogen atoms were fixed to ensure the appropriate neutron

distances of X-H covalent bonds according to Allen & Bruno (2010), and the anisotropic displacement parameters were estimated using the SHADE3 web server. (Madsen & Hoser, 2014) The values for the exponents in the expression of the radial functions for S were set to values (6,6,6,7,7). Several other sets of parameters were also tested, but the best description of electron density was found for the values given above. The local coordinate system was defined so that carbon atoms forming an aromatic ring, chlorine atom and nitrogen atom were given symmetry m perpendicular to z -direction of the local coordinate system. The multipole expansion was truncated at the hexadecapole level for S and Cl atoms, octupole level for the C, N and O atoms and at the dipole level for H atoms (bond directed dipole). For atoms with local symmetry defined to be different than I , only non-zero multipole components were refined. Both κ and ' κ' parameters were refined for Cl and S atoms. For C, N and O atoms, the κ parameter was included. For H atoms, κ and ' κ' parameters were fixed at 1.20 and 1.13, respectively. The refinement of selected anharmonic parameters for Cl and S atoms was necessary. The final data refinement parameters are given in Table S2. The DRK-plot, fractal plot, and the distribution of residual electron density indicates the applied model's correctness (Figure S1).

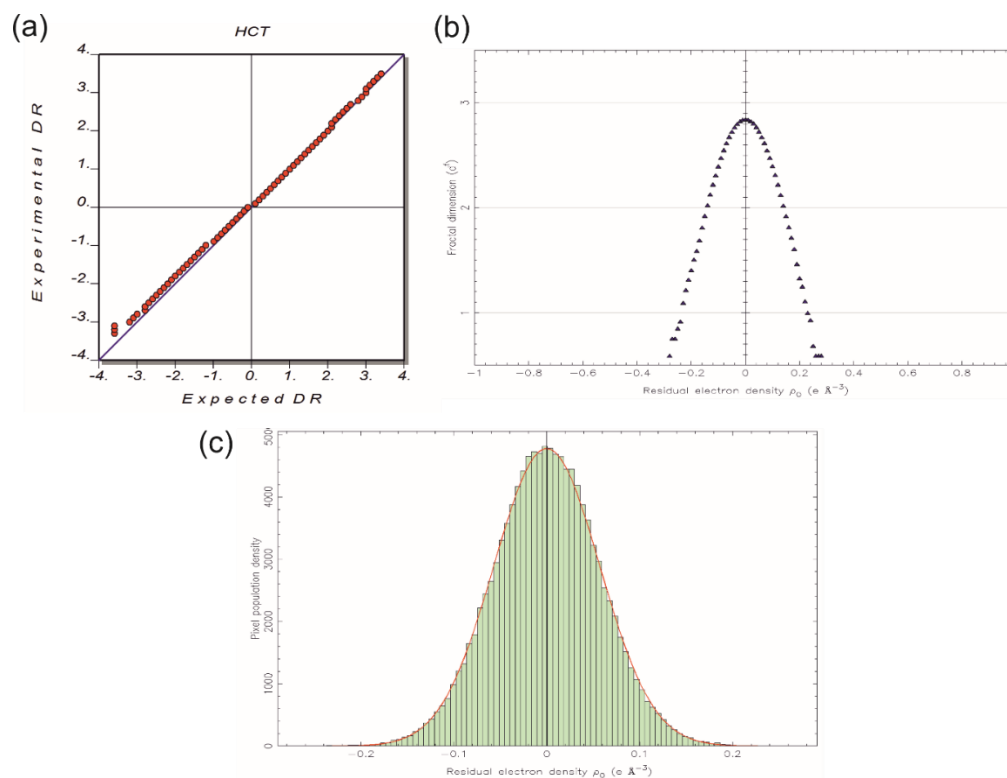


Figure S1 a) DRK-plot, b) fractal plot, and c) the distribution of residual electron density for (I).

Topological analysis of experimental electron density was performed using the XDPROP package implemented in the XD2016 program. The obtained topological parameters were compared with theoretical values calculated as described in section S2.3.

Table S2 Details of the multipolar refinement of (I).

No. of data	5691
No. of data with $I > 2\sigma(I)$	5326
No. of refined parameters	387
$R[I > 2\sigma(I)]/wR(I)/S$	0.0205/ 0.0194/0.996
$\rho_{\max}/\rho_{\min}/\text{rms}$ ($e\text{\AA}^{-3}$)	0.269/-0.316/ 0.055

S2.2. Intramolecular interactions

Experimental and theoretical topological parameters of intramolecular interactions found in (I) are given in Table S3. Despite the optimization of atomic positions for theoretical electron density, most intramolecular interactions have comparable distances, and topological parameters calculated at the position of bond critical points are similar. The most considerable difference in intramolecular distances (ca. 0.08 Å) between theory and experiment is observed for S-O bonds. However, it does not influence the values of topological parameters particularly. The positive sign of the Laplacian at the bond critical point of S-O bonds and $G(r)/\rho > 1$ suggest that it is a highly polarized single bond (Schmøkel *et al.*, 2012; Tantardini *et al.*, 2016; Wojnarska *et al.*, 2018). This type of interaction is difficult to model. This can be a reason for differences in the length of S-O bonds when comparing values from theoretical calculations and experiment.

S2.3. Intermolecular interactions

Topological parameters of intermolecular interactions in (I) are given in Table S4. All theoretically calculated hydrogen bonds of N-H···O type are shorter than those found from experimental electron density. In both datasets the strongest hydrogen bond is N2-H2···O2A[-x+1,y+1/2,-z+1] followed by N2A-H2A2···O1A[-x+1,y+1/2,-z+1] and N1-H1···O2B[-x,y+1/2,-z+1]. There are no significant differences for C-H···O interactions.

Allen, F. H. & Bruno, I. J. (2010). *Acta Cryst. B* **66**, 380–386.

Blessing, R. H. (1997). *J. Appl. Cryst.* **30**, 421-426.

Hansen, N. K. & Coppens, P. (1978). *Acta Cryst. A* **34**, 909–921.

Madsen, A. Ø. & Hoser, A. A. (2014). *J. Appl. Cryst.* **47**, 2100-2104.

Schmøkel, M. S., Cenedese, S., Overgaard, J., Jørgensen, M. R. V., Chen, Y.-S., Gatti, C., Stalke, D. & Iversen, B. B. (2012). *Inorg. Chem.* **51**, 8607–8616.

- Tantardini, C., Boldyreva, E. V. & Benassi, E. (2016) J. Phys. Chem. A 120, 10289–10296.
- Volkov, A., Macchi, P., Farrugia, L. J., Gatti, C., Mallinson, P. R., Richter, T. & Koritsanszky, T. (2016) *XD2016 - a computer program for multipole refinement, topological analysis and evaluation of intermolecular energies from experimental and theoretical structure factors*.
- Wojnarska, J., Gryl, M., Seidler, T. & Stadnicka, K. M. (2018). *CrystEngComm* **20**, 3638–3646.

Table S3 Topological analysis of intramolecular interactions in (I) from theoretical calculations (first row) and experiment (second row). d – intramolecular distance (Å); d_1 , d_2 – distances between bond critical point and interacting atoms (Å), $\rho(r)$ – charge density (a.u.); $\nabla^2\rho(r)$ – Laplacian of electron density (a.u.); $V(r)$, $G(r)$, $E(r)$ – local potential, local kinetic and total energy density (a.u.).

Bond	d	d_1	d_2	$\rho(r)$	$\nabla^2\rho(r)$	λ_1	λ_2	λ_3	ε	$G(r)$	$V(r)$	$E(r)$	$ V(r) /G(r)$	$G(r)/\rho$	$E(r)/\rho$
C4-C1	1.377	0.684	0.693	0.320	-0.92	-0.68	-0.56	0.32	0.21	0.1087	-0.4484	-0.3397	4.13	0.34	-1.06
	1.391	0.656	0.734	0.320	-0.74	-0.69	-0.54	0.49	0.27	0.3067	-0.8002	-0.4920	2.60	0.96	-1.53
C1-C2	1.411	0.694	0.717	0.305	-0.87	-0.65	-0.54	0.33	0.20	0.0928	-0.4029	-0.3101	4.34	0.30	-1.01
	1.417	0.678	0.738	0.313	-0.75	-0.70	-0.55	0.50	0.27	0.2890	-0.7661	-0.4772	2.65	0.92	-1.52
S1-C1	1.765	0.732	1.033	0.214	-0.49	-0.28	-0.27	0.06	0.06	0.0971	-0.3166	-0.2195	3.26	0.45	-1.02
	1.743	0.854	0.889	0.218	-0.40	-0.33	-0.31	0.24	0.05	0.1571	-0.4164	-0.2593	2.65	0.73	-1.18
C2-N1	1.348	0.528	0.820	0.329	-1.05	-0.73	-0.64	0.33	0.15	0.1871	-0.6358	-0.4487	3.40	0.56	-1.36
	1.351	0.579	0.772	0.326	-0.77	-0.73	-0.63	0.59	0.15	0.3142	-0.8209	-0.5068	2.61	0.97	-1.55
S1-N2	1.688	0.668	1.020	0.208	-0.07	-0.29	-0.25	0.47	0.15	0.1873	-0.3923	-0.2050	2.09	0.90	-0.98
	1.644	0.693	0.951	0.225	-0.19	-0.33	-0.29	0.43	0.16	0.2075	-0.4638	-0.2564	2.23	0.92	-1.14
C3-N2	1.472	0.608	0.864	0.253	-0.59	-0.50	-0.48	0.39	0.04	0.1035	-0.354	-0.2505	3.42	0.40	-0.99
	1.464	0.649	0.815	0.262	-0.38	-0.51	-0.49	0.62	0.04	0.2445	-0.5853	-0.3393	2.39	0.94	-1.29
C7-C2	1.409	0.675	0.734	0.307	-0.90	-0.66	-0.56	0.32	0.18	0.0925	-0.4092	-0.3167	4.42	0.30	-1.03
	1.415	0.698	0.716	0.308	-0.73	-0.66	-0.59	0.51	0.12	0.2816	-0.7469	-0.4653	2.65	0.91	-1.51

C4-C5	1.380	0.685	0.695	0.318	-0.91	-0.67	-0.56	0.32	0.21	0.1089	-0.4458	-0.3369	4.09	0.34	-1.05
	1.392	0.684	0.708	0.322	-0.73	-0.68	-0.57	0.52	0.20	0.3127	-0.8076	-0.4949	2.58	0.97	-1.53
S1-O1A	1.513	0.612	0.901	0.242	0.58	-0.36	-0.35	1.28	0.01	0.3777	-0.6109	-0.2332	1.62	1.56	-0.96
	1.438	0.579	0.858	0.299	1.01	-0.45	-0.45	1.92	0.00	0.5542	-0.855	-0.3008	1.54	1.85	-1.00
C7-C6	1.361	0.644	0.717	0.333	-1.00	-0.73	-0.57	0.31	0.28	0.1216	-0.493	-0.3714	4.05	0.36	-1.11
	1.376	0.649	0.727	0.314	-0.70	-0.68	-0.51	0.48	0.34	0.3008	-0.7765	-0.4757	2.58	0.96	-1.51
C5-C6	1.402	0.685	0.717	0.308	-0.88	-0.66	-0.54	0.32	0.21	0.0973	-0.4141	-0.3168	4.26	0.31	-1.02
	1.414	0.673	0.741	0.313	-0.70	-0.68	-0.53	0.52	0.28	0.2993	-0.772	-0.4727	2.57	0.96	-1.51
S2-C5	1.782	0.848	0.934	0.208	-0.56	-0.30	-0.27	0.01	0.10	0.0541	-0.2472	-0.1931	4.57	0.26	-0.92
	1.759	0.861	0.897	0.213	-0.43	-0.35	-0.30	0.23	0.16	0.1467	-0.4001	-0.2534	2.72	0.69	-1.19
C3-N1	1.456	0.597	0.859	0.263	-0.66	-0.55	-0.50	0.38	0.10	0.1077	-0.3812	-0.2735	3.54	0.41	-1.04
	1.449	0.613	0.836	0.256	-0.45	-0.53	-0.48	0.56	0.10	0.2223	-0.5587	-0.3364	2.51	0.87	-1.31
S1-O1B	1.502	0.610	0.892	0.245	0.61	-0.36	-0.34	1.31	0.04	0.3882	-0.6241	-0.2359	1.61	1.58	-0.96
	1.432	0.580	0.852	0.298	1.02	-0.45	-0.45	1.92	0.0	0.5527	-0.8506	-0.2964	1.53	1.85	-0.99
C6-Cl6	1.778	0.798	0.980	0.176	-0.2	-0.27	-0.25	0.32	0.06	0.0608	-0.1706	-0.1098	2.81	0.34	-0.62
	1.725	0.801	0.924	0.206	-0.06	-0.35	-0.3	0.59	0.16	0.1956	-0.406	-0.2104	2.07	0.95	-1.02
S2-O2A	1.515	0.612	0.903	0.241	0.56	-0.35	-0.35	1.27	0.01	0.3728	-0.6047	-0.2319	1.62	1.54	-0.96
	1.442	0.582	0.860	0.302	0.89	-0.44	-0.42	1.75	0.05	0.5379	-0.8535	-0.3156	1.58	1.78	-1.04

S2-N2A	1.636	0.647	0.989	0.219	0.07	-0.32	-0.27	0.66	0.19	0.2333	-0.4482	-0.2149	1.92	1.06	-0.98
	1.599	0.665	0.934	0.237	-0.16	-0.37	-0.31	0.51	0.2	0.2326	-0.5068	-0.2741	2.17	0.98	-1.15
S2-O2B	1.506	0.609	0.897	0.244	0.61	-0.36	-0.35	1.33	0.03	0.3884	-0.6237	-0.2353	1.61	1.59	-0.96
	1.435	0.580	0.855	0.302	0.95	-0.48	-0.43	1.85	0.12	0.5483	-0.861	-0.3127	1.57	1.81	-1.03

Table S4 Topological analysis of hydrogen bonds in (I) from theoretical calculations (first row) and experiment (second row). d – intramolecular distance (Å); d_1 , d_2 – distances between bond critical point and interacting atoms (Å), $\rho(r)$ – charge density (a.u.); $\nabla^2\rho(r)$ – Laplacian of electron density (a.u.); $V(r)$, $G(r)$, $E(r)$ – local potential, local kinetic and total energy density (a.u.).

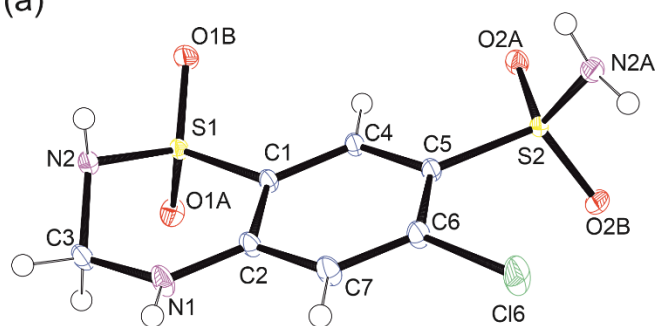
Bond	d	d_1	d_2	$\rho(r)$	$\nabla^2\rho(r)$	λ_1	λ_2	λ_3	ϵ	$G(r)$	$V(r)$	$E(r)$
C7-H7···O1B ^{iv}	2.404	1.018	1.386	0.011	0.04	-0.01	-0.01	0.06	0.25	0.0089	-0.007	0.0019
	2.331	0.970	1.361	0.012	0.05	-0.01	-0.01	0.07	0.06	0.0104	-0.0074	0.003
N2A-H2A2···O1A ⁱⁱ	1.835	0.641	1.194	0.031	0.12	-0.04	-0.04	0.21	0.01	0.0277	-0.0261	0.0016
	1.908	0.685	1.223	0.018	0.13	-0.03	-0.02	0.18	0.05	0.0252	-0.0178	0.0074
C3-H3A···O1A ^v	2.436	0.981	1.455	0.008	0.03	-0.01	-0.01	0.05	0.07	0.0063	-0.0046	0.0017
	2.437	0.876	1.561	0.002	0.04	-0.002	-0.002	0.04	0.22	0.0059	-0.0030	0.0029
N2A-H2A1···N2 ⁱ	2.140	0.750	1.390	0.019	0.06	-0.02	-0.02	0.11	0.03	0.0131	-0.0109	0.0022
	2.346	0.849	1.496	0.006	0.06	-0.01	-0.01	0.07	0.16	0.0104	-0.0059	0.0044
N2-H2···O2A ⁱⁱ	1.745	0.594	1.151	0.039	0.13	-0.06	-0.06	0.26	0.03	0.0349	-0.0369	-0.002

	1.853	0.651	1.201	0.018	0.16	-0.02	-0.02	0.20	0.05	0.0296	-0.0193	0.0104
N1-H1 \cdots O2B ⁱⁱⁱ	1.841	0.652	1.189	0.028	0.12	-0.04	-0.04	0.20	0.0	0.0265	-0.024	0.0025
	1.988	0.711	1.277	0.015	0.09	-0.02	-0.02	0.14	0.06	0.0178	-0.0133	0.0044

Symmetry codes: i [x,y,z+1]; ii[-x+1,y+1/2,-z+1]; iii[-x,y+1/2,-z+1]; iv[x-1,y,z]; v[-x,y+1/2,-z]

S3. Description of crystal structures

(a)



(b)

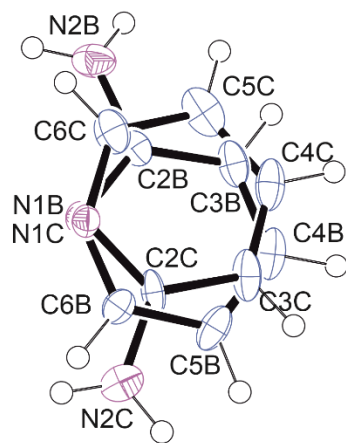
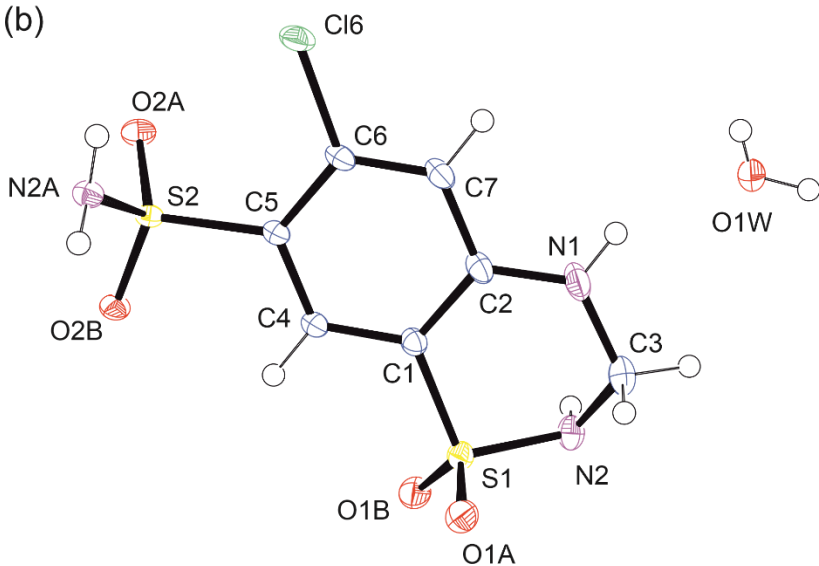


Figure S2 The asymmetric unit of (I) (a) and (II) (b) with atom numbering schemes. 2-aminopyridine is disordered over two positions with site occupancy factors of 83% (B) and 17% (C). Atoms are represented by the displacement ellipsoids drawn at a 50% probability level. The drawing was prepared using Ortep-3 (L. J. Farrugia, *J. Appl. Cryst.* (2012), 45, 849-854).

Table S5 Experimental geometry of hydrogen bonds in (I) (\AA , $^\circ$).

	H \cdots A	D \cdots A	DHA
N2A-H2A1 \cdots N2 ⁱ	2.45(1)	3.294(2)	160(1)
N2A-H2A2 \cdots O1A ⁱⁱ	2.04(1)	2.891(1)	164(2)
N1-H1 \cdots O2B ⁱⁱⁱ	2.10(1)	2.893(1)	152(2)
N2-H2 \cdots O2A ⁱⁱ	2.00(1)	2.880(1)	178(2)
C7-H7 \cdots O1B ^{iv}	2.43	3.125(2)	130
C3-H3A \cdots O1A ^v	2.49	3.471(2)	172

Symmetry codes: i [x,y,z+1]; ii[-x+1,y+1/2,-z+1]; iii[-x,y+1/2,-z+1]; iv[x-1,y,z]; v[-x,y+1/2,-z]

Table S6 Experimental geometry of hydrogen bonds in (II) (\AA , $^\circ$).

	H \cdots A	D \cdots A	DHA
N2A-H2A1 \cdots O2B ⁱ	2.09(2)	2.910(2)	160(1)
N2A-H2A2 \cdots O2A ⁱⁱ	2.22(2)	2.991(2)	164(1)
O1W-H1W1 \cdots N1B	1.80(1)	2.651(2)	177(1)
O1W-H1W1 \cdots N1C	1.89(1)	2.743(2)	178(1)
O1W-H1W2 \cdots O1A ⁱⁱⁱ	2.21(1)	2.876(2)	136(1)
N2-H2 \cdots O1W ^{iv}	1.98(1)	2.854(2)	165(2)
C7-H7 \cdots O1A ⁱⁱⁱ	2.50	3.418(2)	162
N1-H1 \cdots O1W	2.07(2)	2.827(2)	146(2)
N2B-H2B1 \cdots O1B ^v	2.20(2)	2.959(2)	143(2)
N2B-H2B2 \cdots N2 ⁱⁱⁱ	2.61(2)	3.459(2)	161(2)
N2C-H2C1 \cdots O1A ^{vi}	2.57(2)	3.133(2)	123(2)
C5B-H5B \cdots O2A ^{vii}	2.58	3.445(2)	151
C5C-H5C \cdots N2C ^{vi}	2.57	3.133(2)	124

Symmetry codes: i [-x+1/2,y+1/2,z-1/2]; ii[-x+1/2,y+1/2,z+1/2]; iii[x,y,z-1]; iv[-x+1,-y+1,z+1/2]; v[-x+1,-y+1,z-3/2]; vi[-x+1,-y+2,z-1/2]; vii[x+1/2,-y+3/2,z]

S4. Optical properties of studied materials

Table S7 $\chi^{(2)}$ tensor components for (I) (values in pm/V), as calculated at the MP2 level.

method	λ/nm	$\chi^{(2)}_{112}$	$\chi^{(2)}_{211}$	$\chi^{(2)}_{222}$	$\chi^{(2)}_{123}$	$\chi^{(2)}_{213}$	$\chi^{(2)}_{312}$	$\chi^{(2)}_{233}$	$\chi^{(2)}_{323}$
LFT	∞	0.4		-0.8	1.1			-4.1	
	1064	0.5	0.4	-0.9	1.5	1.5	1.3	-5.5	-5.9
Q-LFT	∞	0.4		-0.7	1.1			-3.8	
	1064	0.5	0.5	-0.8	1.4	1.5	1.3	-5.1	-5.3

Table S8 $\chi^{(2)}$ tensor components for (II) (values in pm/V), as calculated at the MP2 level.

method	λ/nm	$\chi^{(2)}_{113}$	$\chi^{(2)}_{311}$	$\chi^{(2)}_{223}$	$\chi^{(2)}_{322}$	$\chi^{(2)}_{333}$
LFT	∞	-4.1		-0.4		-1.8
	1064	-5.3	-5.0	-0.7	-0.7	-2.6
Q-LFT	∞	-3.8		-0.2		-1.6
	1064	-4.9	-4.7	-0.4	-0.4	-2.4

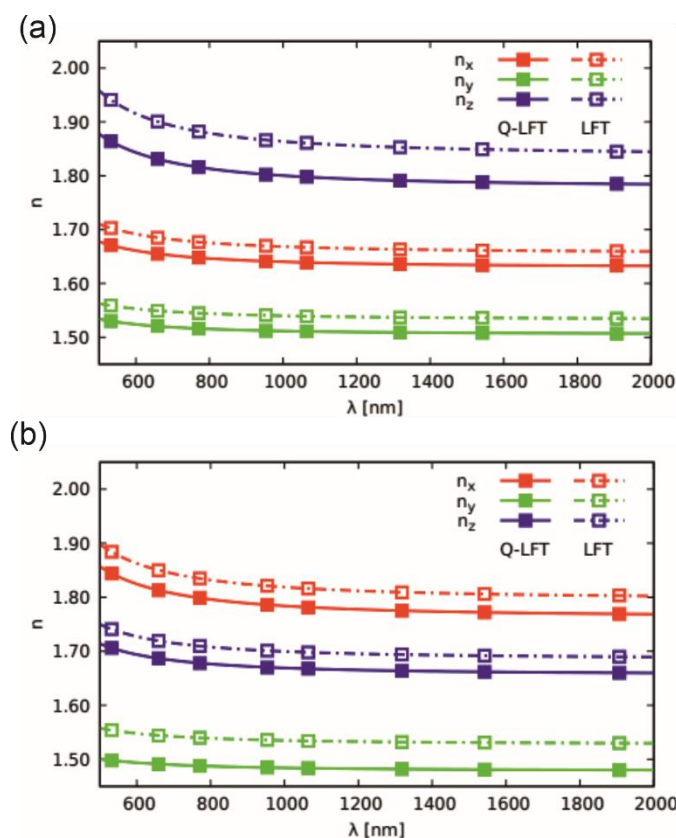


Figure S3 Dispersion of the refractive indices calculated at the MP2 level in LFT and Q-LFT approximations for (a) (I) and (b) (II).

S5. Statistical analysis of CSD Database

The search of the CSD database (version 5.41) has been performed to examine tendency of primary and secondary sulfonamide groups to form intermolecular interactions with other sulfonamide groups.

In the first step, all multicomponent materials containing hydrochlorothiazide molecule were searched using following parameters: $R \leq 0.75$, with 3D coordinates, no errors, no polymeric structures, only single crystal data. In total, 22 unique crystal structures were found. In each of them, intermolecular interactions between 1) two primary sulfonamide groups ($P \cdots P$), 2) primary sulfonamide group and non-sulfonamide crystal component ($P \cdots C$), 3) two secondary sulfonamide groups ($S \cdots S$), 4) secondary sulfonamide group and non-sulfonamide crystal component ($S \cdots C$) and 5) primary and secondary sulfonamide groups ($P \cdots S$) were checked (Table S9). There were no cases in which the secondary sulfonamide group formed intermolecular interactions with another crystal building block, while no interactions between the primary sulfonamide group and other molecules were present. However, in none of the 22 crystal structures, there were intermolecular interactions between

two secondary sulfonamides. In 6 crystal structures interactions between two primary sulfonamide groups were observed. In conclusion, the primary sulfonamide group has a higher tendency to interact with other sulfonamide groups than the secondary one. To confirm the observation derived from the analysis of the crystal structures containing hydrochlorothiazide molecule, the CSD database was searched for crystal structures containing primary or secondary sulfonamide group (search parameters: $R \leq 0.75$, with 3D coordinates, no errors, no polymeric structures, only single crystal data).

Among the found structures, we observed at least one intermolecular interaction of $N\text{-H}\cdots O$ type was present in the 62% crystal structures containing molecules with the primary sulfonamide group (Table S10). This percentage is similar to that found for multicomponent materials (60%). In the case of the secondary sulfonamide group, at least one interaction between sulfonamide groups was found in 44% of searched crystal structures. The number of structures further decreased (21%) when only multicomponent materials containing at least one molecule with a secondary sulfonamide group was analysed. These results indicate that primary sulfonamides have a higher tendency to form intermolecular interactions with another sulfonamide group than secondary sulfonamides.

Table S9 The presence of intermolecular interactions formed between two primary sulfonamide groups ($P\cdots P$), primary sulfonamide group and another crystal component ($P\cdots C$), two secondary sulfonamide groups ($S\cdots S$), secondary sulfonamide group and another crystal component ($S\cdots C$) and primary and secondary sulfonamide groups ($P\cdots S$) observed in the reported multicomponent materials containing hydrochlorothiazide molecule.

REFCODE	$P\cdots P$	$P\cdots C$	$S\cdots S$	$S\cdots C$	$P\cdots S$
CASCAB	-	+	-	+	-
CASMAL	+	+	-	+	+
DADMED	-	+	-	+	-
DADMIH	+	+	-	-	+
DADMUT	-	+	-	+	-
DADNAA	-	-	-	-	+
DADNEE	-	+	-	+	+
EGENIP02	-	+	-	+	-
EGENOV	-	+	-	+	-
EGENUB	+	+	-	+	-

MUPPIX	-	+	-	+	-
NOLBOI	-	+	-	+	+
NOLCAV	-	+	-	-	+
NOLCEZ	-	+	-	+	-
ODATIX	-	+	-	-	+
ODEFEJ	+	+	-	-	-
PIRLUZ	-	+	-	+	+
PIRXOF	+	+	-	+	-
PIRXUL	-	+	-	+	-
PIRYAS	+	+	-	+	+
SIZZUS	-	+	-	+	+
VITWIE	-	+	-	+	-

Table S10 Statistical analysis of intermolecular interactions found between sulfonamide groups in crystal structures containing the primary or secondary sulfonamide group

Crystal structures containing molecule with:	Total number of crystal structures	Total number of crystal structures with N-H···O intermolecular interactions	Total number of multicomponent materials	Total number of multicomponent material's with N-H···O intermolecular interactions
Primary sulfonamide group	687	425	314	187
Secondary sulfonamide group	4364	1921	763	162